

## Adiabatic processes in three-level systems

Timo A. Laine and Stig Stenholm\*

*Research Institute for Theoretical Physics, P.O. Box 9, FIN-00014, University of Helsinki, Finland*

(Received 5 September 1995)

In this paper we consider the adiabatic transfer in three-level systems using the counterintuitive pulse sequence, the stimulated Raman process (STIRAP). We consider explicitly the nonadiabatic corrections to the ideal case. The problem simplifies when we use certain pulse types extending to infinity, ramp pulses. In this case we find models which are analytically solvable. In the smooth pulse case, we find simple exponential corrections to adiabatic behavior. For a resonant intermediate level, the problem is equivalent to a two-level problem, where adiabatic corrections have been investigated extensively. We utilize these results to interpret the behavior of the three-level system exposed to the counterintuitive pulse case. When the pulse separation is in a certain range, exponential adiabatic behavior is found, and the numerical data can be explained by the analytic theory taken from the two-level work. We cannot explain all results analytically, but the computations suggest that this description of the three-level system gives a good understanding of the STIRAP.

PACS number(s): 32.80.Bx

### I. INTRODUCTION

The three-level problem has played a central role in the development of laser spectroscopy and quantum optics. Use of coherent tunable light sources has made it possible to utilize this configuration to achieve many goals in high-precision spectroscopy and the investigations of laser-induced coherence. With the development of well-controlled light pulses, new coherent transient and population transfer phenomena have become available.

Among the three-level phenomena, the appearance of adiabatic population transfer offered a new and unexpected effect. In the transient but adiabatic limit, population can be transferred from an initial level to a final one without any losses to the virtual intermediate level, which never acquires an appreciable occupation. The process is superior to any other scheme; the use of two consecutive  $\pi$  pulses serve the same purpose, but the result is sensitive to the exact pulse areas and decay and perturbations of the intermediate level, through which the whole population has to pass. In the stimulated Raman process (STIRAP) the two initially unoccupied levels are coupled first, and the initially occupied level is emptied only by a later pulse. This *counterintuitive* pulse sequence contrasts strongly with the ordinary consecutive coherent transfer. However, the STIRAP works perfectly in the adiabatic limit, its efficiency is totally unaffected by perturbations of the virtual intermediate state, and it lacks sensitivity to the intermediate detuning and the pulse amplitudes. The initial and final levels have to be in resonance to satisfy energy conservation in the transfer. This is the only strict condition to be put on an experimental setup; other parameters may vary over considerable ranges in the sample.

The adiabatic three-level situation was investigated early by Hioe and collaborators [1,2]. Later, in a series of papers, Carroll and Hioe [3–6] exploited many of the properties of such systems. Only around 1990 did Bergmann and his collaborators take a serious look at the possibility of utilizing the process in realistic physical systems [7–12]. Experi-

mental realizations have been achieved in [13–15]. The adiabatic process is further discussed by Danileiko, Romanenko, and Yatsenko [16], the possible extension to continuous sets of intermediate levels is criticized by Nakajima *et al.* [17], and superadiabatic transformations are applied to the system by Elk [18].

Many of the theoretical investigations have used the ideal adiabatic limit for the theoretical treatment and investigated the imperfect situation numerically. Here we want to look at the nonadiabatic corrections and try to find analytic expressions for these corrections close to the adiabatic limit. Such investigations have been carried out over many decades for the corresponding two-level situation; for a recent review, consult [19]. Here we try to combine known adiabatic methods with detailed numerical investigations to gain insight into the adiabatic asymptotics of three-level systems.

We start by formulating the problem in the adiabatic basis, and we describe the properties of this system in Sec. II A. When the intermediate process is exactly at resonance, i.e., the detuning is zero, the problem simplifies. In our treatment we utilize this property to simplify both analytical and numerical processes. As the value of the detuning is irrelevant in the ideal adiabatic limit, we feel that valuable results can be obtained even in this case. Naturally, it would be extremely interesting to gain insight into the dependence of the nonadiabatic corrections on the value of the detuning. For large detunings, we expect the process to become more coherent, and it is actually possible that increasing the detuning will make the population transfer more efficient. This, however, will be considered in future work.

With a resonant intermediate state, the three-level problem can be mapped uniquely onto an associated two-level problem. This was pointed out by Carroll and Hioe in [6], even if the procedure rests on a well-known group theoretic relation [20]. This relationship is described in Sec. II B. We use this correspondence to relate our three-level problems to results derived earlier for two-level systems.

In Sec. III, we use the property that pulses that couple unpopulated levels can be modified at will to simplify the adiabatic transfer situation. In Sec. III A, we illustrate the use of such ramp pulses by devising a nonanalytic but trivially

\*Also at Academy of Finland.

solvable model. As this contains discontinuities in the derivatives, the nonadiabatic contributions are dominated by these points, as explained by Berry in a different context [21]. As a realistic model this cannot serve, but it does illustrate the general ideas of the ramp pulses. A similar two-level model was introduced early by Ramsay and Schwinger; see the discussion in [22].

When we make an analytic ramp pulse in Sec. III B, it turns out that this is associated with an exactly solvable two-level problem. This provides us with the solution to a non-trivial case of the STIRAP process. In the adiabatic limit, this displays an exponential dependence on the adiabaticity parameter. Such behavior is well known from the theory of two-level transitions (see [19]) and suggests the use of the corresponding analytic machinery. We adopt the results of the theoretical treatment of Davis and Pechukas [23] and investigate its applicability to the STIRAP situation. To this end we consider the case of separated pulses applied to the system in the counterintuitive sequence. In Sec. IV A we formulate some general results and introduce the analytic approximations from the adiabatic theory of two-level systems. This is done *ad hoc*, without any attempt to justify the results; here we only want to investigate whether they are relevant at all. The generalization to a three-level configuration introduced by Pechukas himself [24] seems to carry no implications for the STIRAP situation.

In Sec. IV B, we look at the case of Gaussian pulses, which is nearly exclusively used in the earlier theoretical investigations. When the pulses are well separated but still overlapping considerably, we do indeed find an exponential region that can be fitted with the Davis-Pechukas formula. For pulses sitting too much on top of each other, the coherent evolution dominates, and this will end the range of the exponential behavior for large adiabaticity parameters. When the pulses are too far separated, no adiabatic transfer takes place, as is easily understood. This shows that the pulse overlap is a suitable measure of the adiabaticity of the system. In certain cases, the nonadiabatic corrections show an exponential dependence on this parameter, but for too large values the behavior breaks down.

To investigate the universality of the results we obtained using Gaussian pulses, we apply the same considerations to the hyperbolic secant pulse shape in Sec. IV C. The numerical work becomes harder and pulse tails decay more slowly, but the same conclusions can be reached. In Sec. IV D, we summarize these conclusions and discover a simple analytic description of the crossover between exponential and coherent behavior in the STIRAP process. This result is entirely based on our numerical work, and no theoretical explanation has been found.

The results are discussed and summarized in Sec. V. We find that the two-level cases associated with the STIRAP process belong to a class not previously considered. The corresponding  $2 \times 2$  Hamiltonian vanishes at both  $\pm \infty$  in time, and hence the energy levels become degenerate both in the initial and in the final situations. The nonadiabatic transfer between the levels takes place when the adiabatic energies are separated. Such systems show the same behavior as our three-level cases, and some of the unexpected features found in this work may well be of interest also for two levels. We

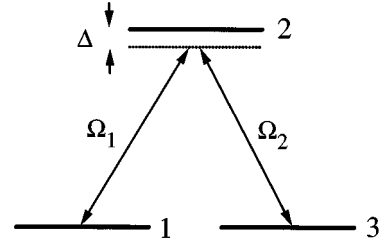


FIG. 1. The three-level system coupled by the time-dependent pulse amplitudes  $\Omega_1$  and  $\Omega_2$ . The population is initially on level 1. The counterintuitive sequence consists in  $\Omega_2$  coming on before the pulse  $\Omega_1$ . The detuning of the intermediate level is  $\Delta$ .

conclude the paper by stressing the need for further works on this aspect of the problem.

## II. ADIABATIC BASES

### A. Three-level system

We consider a three-level system where the levels are coupled in the sequence  $1 \rightarrow 2 \rightarrow 3$ , and no direct coupling between levels 1 and 3 is introduced. Levels 1 and 3 are assumed to be in resonance, but within the rotating-wave approximation the intermediate level may be detuned by the amount  $\Delta$ ; see Fig. 1.

The Hamiltonian for the system is now of the form

$$H = \begin{bmatrix} 0 & \Omega_1(t) & 0 \\ \Omega_1(t) & \Delta & \Omega_2(t) \\ 0 & \Omega_2(t) & 0 \end{bmatrix}, \quad (2.1)$$

where the coupling Rabi amplitudes  $\Omega_{1,2}$  are taken to depend on time. The state vector is written as

$$|\Psi\rangle = c_1|1\rangle + c_2|2\rangle + c_3|3\rangle. \quad (2.2)$$

With this notation we assume the initial condition  $c_1(t_0) = 1$ , and the other two equal zero. The question is how much population can be transferred to the coefficient  $c_3$  at large times. The initial conditions are, in analytic calculations, set at  $t_0 = -\infty$ .

We introduce a unitary transformation  $U$  of the state (2.2)

$$|\Psi\rangle = U|\Phi\rangle \quad (2.3)$$

such that it diagonalizes the Hamiltonian

$$U^\dagger H U = D, \quad (2.4)$$

where  $D$  is the diagonal form of the Hamiltonian.

Writing the unitary transformation in the form

$$U = \begin{bmatrix} \sin\varphi \sin\theta & \cos\theta & \cos\varphi \sin\theta \\ \cos\varphi & 0 & -\sin\varphi \\ \sin\varphi \cos\theta & -\sin\theta & \cos\varphi \cos\theta \end{bmatrix}, \quad (2.5)$$

we find that the new basis vectors  $\{|a_+\rangle, |a_0\rangle, |a_-\rangle\}$  for the state  $|\Phi\rangle$  correspond to the eigenvalues  $\{w_+, 0, w_-\}$ , respectively, where

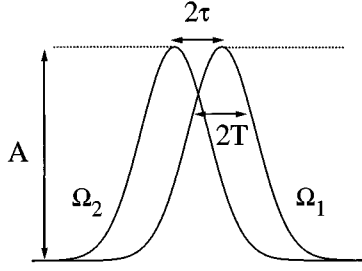


FIG. 2. The pulse sequence in the case of separated pulses (solid lines). Each pulse has a duration  $2T$  and an amplitude  $A$ . The peaks of the pulses are separated by  $2\tau$ . Because initially  $\Omega_2$  and finally  $\Omega_1$  couple ideally unpopulated levels, the adiabatic process is not changed if the pulses are extended to infinite times in the manner indicated by the dotted lines; these are the ramp pulses.

$$w_+ = \Omega_0 \cot \varphi = \frac{1}{2} (\Delta + \sqrt{\Delta^2 + 4\Omega_0^2}), \quad (2.6)$$

$$w_- = -\Omega_0 \tan \varphi = \frac{1}{2} (\Delta - \sqrt{\Delta^2 + 4\Omega_0^2}),$$

and

$$\Omega_0^2 = \Omega_1^2(t) + \Omega_2^2(t). \quad (2.7)$$

The diagonalization requires that the angles in Eq. (2.5) satisfy the relations

$$\begin{aligned} \tan \theta &= \frac{\Omega_1(t)}{\Omega_2(t)}, \\ \tan 2\varphi &= \frac{2\Omega_0(t)}{\Delta}. \end{aligned} \quad (2.8)$$

The state corresponding to the zero eigenvalue is of the form

$$|a_0\rangle = \cos \theta |1\rangle - \sin \theta |3\rangle. \quad (2.9)$$

If we assume the counterintuitive pulse sequence used in the STIRAP experiments we have

$$\begin{aligned} \lim_{t \rightarrow -\infty} \frac{\Omega_1(t)}{\Omega_2(t)} &= 0, \quad \theta \rightarrow 0, \\ \lim_{t \rightarrow +\infty} \frac{\Omega_2(t)}{\Omega_1(t)} &= 0, \quad \theta \rightarrow \frac{\pi}{2}. \end{aligned} \quad (2.10)$$

With these results, we can see that the state (2.9) is  $|1\rangle$  initially and goes to  $-|3\rangle$  finally. If the time-dependent change is introduced slowly enough, the population remains in the state  $|a_0\rangle$  and is adiabatically transferred totally to the state  $|3\rangle$ ; this is the STIRAP. We notice that the process does not depend on the behavior of  $\lim_{t \rightarrow +\infty} \Omega_1(t)$  and  $\lim_{t \rightarrow -\infty} \Omega_2(t)$ , as these functions couple ideally empty levels. In particular, the functions may go to constant values; see the behavior in Fig. 2. Pulses where  $\lim_{t \rightarrow +\infty} \Omega_1(t)$  and  $\lim_{t \rightarrow -\infty} \Omega_2(t)$  are constant values are called *ramp pulses* in this paper. In the adiabatic limit, they act exactly like the ordinary *separated pulses*, which go to zero at  $t = \pm\infty$ .

The explicit time dependence of the Hamiltonian introduces a correction to the diagonal operator (2.4). The state in Eq. (2.3) obeys the transformed Schrödinger equation

$$i \frac{\partial}{\partial t} |\Phi\rangle = \left( D - iU^\dagger \frac{\partial}{\partial t} U \right) |\Phi\rangle. \quad (2.11)$$

With the unitary matrix (2.5), we obtain the adiabatic form of the Hamiltonian

$$\begin{aligned} H_{\text{ad}} &\equiv \left( D - iU^\dagger \frac{\partial}{\partial t} U \right) \\ &= \begin{bmatrix} \Omega_0 \cot \varphi & i\dot{\theta} \sin \varphi & i\dot{\varphi} \\ -i\dot{\theta} \sin \varphi & 0 & -i\dot{\theta} \cos \varphi \\ -i\dot{\varphi} & i\dot{\theta} \cos \varphi & -\Omega_0 \tan \varphi \end{bmatrix}, \end{aligned} \quad (2.12)$$

where we have

$$\dot{\theta} = \frac{\dot{\Omega}_1 \Omega_2 - \dot{\Omega}_2 \Omega_1}{\Omega_0^2}, \quad (2.13)$$

$$\dot{\varphi} = \Delta \frac{\dot{\Omega}_1 \Omega_1 + \dot{\Omega}_2 \Omega_2}{\Omega_0 (\Delta^2 + 4\Omega_0^2)} = \frac{\Delta \dot{\Omega}_0}{(\Delta^2 + 4\Omega_0^2)}.$$

At resonance,  $\Delta = 0$ ; we find from Eq. (2.8) that the angle  $\varphi = \pi/4$ . According to Eq. (2.13) it stays constant. However, the same happens if  $\Omega_0$  in Eq. (2.7) does not depend on time. This can be achieved retaining the adiabatic population transfer because of the argument illustrated in Fig. 2. In this case we can use the detuning  $\Delta$  to fix the angle at an arbitrary value; see Eq. (2.8). The choice  $\Delta = 0$  is still convenient because then  $\cos \varphi = \sin \varphi$ .

If the two pulses are roughly of equal magnitude,  $\Omega_1 \sim \Omega_2$ , we can see that the nonadiabatic coupling  $\dot{\theta}$  in Eq. (2.13) is independent of the pulse amplitude and inversely proportional to the time scale  $T$  of the variation of the pulse shape. This is a universal feature of all systems under consideration. We will look at a series of models for the STIRAP situation, which are chosen to illuminate the various features of the physics of the process.

## B. Associated two-level problem

In the resonant case,  $\Delta = 0$ , we find that the parameters from Eq. (2.2) can be chosen such that  $c_1$  and  $c_3$  are real and  $c_2$  purely imaginary. With normalization, this leaves two free parameters only. This suggests that the dynamics takes place in a space of lower dimensions than three; two turns out to be a good choice. In that case we start from four real parameters, but the overall phase and the normalization reduce the degrees of freedom to the same number as in the three-level case. We look closer at this relationship.

We start by considering the conventional two-level problem

$$i \frac{\partial}{\partial t} \begin{bmatrix} d_1 \\ d_2 \end{bmatrix} = \frac{1}{2} \begin{bmatrix} -\Omega_0 & -i\sqrt{2}\gamma \\ i\sqrt{2}\gamma & \Omega_0 \end{bmatrix} \begin{bmatrix} d_1 \\ d_2 \end{bmatrix}. \quad (2.14)$$

Here we assume that, in the general case, both  $\Omega_0$  and  $\gamma$  may depend on time. Problems of this type have been discussed in quantum mechanics for a long time [19]. Here we use this problem as a point of reference for our work on the three-level case. In addition to the equation of motion (2.14) we assume the initial condition characteristic of many population transfer problems,

$$\begin{aligned} d_1(t_0) &= 1, \\ d_2(t_0) &= 0. \end{aligned} \quad (2.15)$$

In most cases  $t_0 = -\infty$ .

Starting with the state vector in (2.14), we now define new variables

$$\begin{aligned} r_+ &= \sqrt{2}d_1^*d_2, \\ r_- &= \sqrt{2}d_1d_2^*, \\ r_0 &= |d_1|^2 - |d_2|^2. \end{aligned} \quad (2.16)$$

The initial conditions (2.15) translate directly into the equivalent set

$$\begin{aligned} r_+(t_0) &= r_-(t_0) = 0, \\ r_0(t_0) &= 1. \end{aligned} \quad (2.17)$$

Using Eq. (2.14) to calculate the equation of motion for the components  $\{r_+, r_0, r_-\}$ , we find

$$i\frac{\partial}{\partial t} \begin{bmatrix} r_+ \\ r_0 \\ r_- \end{bmatrix} = \begin{bmatrix} \Omega_0 & i\gamma & 0 \\ -i\gamma & 0 & -i\gamma \\ 0 & i\gamma & -\Omega_0 \end{bmatrix} \begin{bmatrix} r_+ \\ r_0 \\ r_- \end{bmatrix}. \quad (2.18)$$

If we set

$$\gamma = \frac{\dot{\theta}}{\sqrt{2}}, \quad (2.19)$$

Eq. (2.18) is exactly of the form Eq. (2.12), when we set  $\varphi = \pi/4$ . However, the result (2.18) is equivalent to Eq. (2.14) for arbitrary time dependence of the parameters. We have carried out the correspondence in the adiabatic basis, where it turns out to be convenient to work. However, the form (2.14) together with the definitions (2.7) and (2.13) show (2.14) to be the adiabatic representation of the bare two-level system,

$$H_{2d} = \frac{1}{2} \begin{bmatrix} \Omega_2 & \Omega_1 \\ \Omega_1 & -\Omega_2 \end{bmatrix}. \quad (2.20)$$

This relationship was pointed out by Carroll and Hioe [6]. It is a straightforward application of the well-known SU(2) representation of the rotation group; see Ref. [20]. With only three real parameters characterizing the state, the unitary transformations of quantum theory are equivalent with simple rotations. For convenience, we choose the phases in Eq. (2.16) different from the standard convention.

When we have solved the two-level system (2.14), we immediately have the solution of the corresponding three-

level system (2.18). Such a one-to-one relation between the solutions holds only for restricted sets of initial conditions. In this special case, the number of independent components in the problem (2.18) is small enough to be represented by the two-level system. Using the definition (2.16), we can verify the conservation of probability in the form

$$|r_+|^2 + |r_-|^2 + |r_0|^2 = (|d_1|^2 + |d_2|^2)^2. \quad (2.21)$$

Thus we find that if the two-level state is normalized, so is the three-level state.

Using the relations (2.3) and (2.5) to express the original state vector  $|\Psi\rangle$  in terms of the components of the two-level system, we find

$$\begin{aligned} c_1 &= \sin\theta(d_1^*d_2 + d_1d_2^*) + \cos\theta(|d_1|^2 - |d_2|^2), \\ c_2 &= (d_1^*d_2 - d_1d_2^*), \\ c_3 &= \cos\theta(d_1^*d_2 + d_1d_2^*) - \sin\theta(|d_1|^2 - |d_2|^2). \end{aligned} \quad (2.22)$$

Following from the discussion of Eqs. (2.9) and (2.10), we see that the final population on level  $|3\rangle$  becomes, according to Eq. (2.22),

$$|c_3(\infty)|^2 = [ |d_1(\infty)|^2 - |d_2(\infty)|^2 ]^2 = [ 2|d_2(\infty)|^2 - 1 ]^2. \quad (2.23)$$

### III. RAMP PULSES

#### A. Nonanalytic model

In this section, we first introduce a rather artificial model, which displays the main features of the situation but allows simple analytic evaluation of all quantities. It is not supposed to correspond to any realistic physical experiment.

We define the two coupling amplitudes in the following way:

$$\Omega_1(t) = \begin{cases} 0; & t \leq -\frac{T}{2} \\ A \sin\left[\frac{\pi}{2}\left(\frac{t}{T} + \frac{1}{2}\right)\right]; & -\frac{T}{2} \leq t < \frac{T}{2} \\ A; & \frac{T}{2} \leq t, \end{cases} \quad (3.1)$$

$$\Omega_2(t) = \begin{cases} A; & t \leq -\frac{T}{2} \\ A \cos\left[\frac{\pi}{2}\left(\frac{t}{T} + \frac{1}{2}\right)\right]; & -\frac{T}{2} \leq t < \frac{T}{2} \\ 0; & \frac{T}{2} \leq t. \end{cases} \quad (3.2)$$

These pulses are continuous but have jumps in their derivatives. The behavior is shown in Fig. 3, and it is easily seen that for *all times* the amplitude stays constant,  $\Omega_0 = A$ . We choose  $\varphi = (\pi/4)$  ( $\Delta = 0$ ). The nonadiabatic coupling  $\dot{\theta}$  is zero except inside the interval  $-(T/2) \leq t < T/2$ , where it becomes the constant

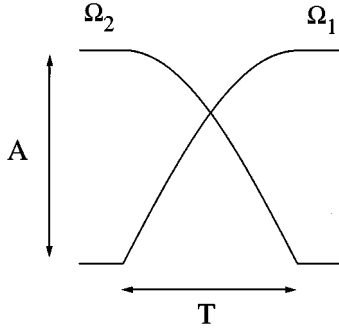


FIG. 3. When the ramp pulses are constructed from trigonometric sections fitted to constant lines, we obtain the pulse behavior shown in this figure. We notice that both the first and the second derivatives are discontinuous.

$$\dot{\theta} = \frac{\pi}{2T} \equiv \sqrt{2}\gamma. \quad (3.3)$$

With this, the adiabatic Hamiltonian (2.12) becomes the constant matrix

$$H_{\text{ad}} = \begin{bmatrix} A & i\gamma & 0 \\ -i\gamma & 0 & -i\gamma \\ 0 & i\gamma & -A \end{bmatrix}. \quad (3.4)$$

This problem can directly be solved over the range  $-(T/2) \leq t < T/2$ ; outside this range the coupling is zero and no further transfer of population takes place.

From dimensional arguments, we conclude that the solution can only depend on the combination  $AT$ , and we define the parameter  $\eta$  by setting

$$\sinh \eta = \frac{\pi}{2AT}. \quad (3.5)$$

In the adiabatic limit,  $AT \rightarrow \infty$ , the parameter  $\eta$  goes to zero as  $(AT)^{-1}$ .

The solution at  $t = T/2$  is

$$\begin{aligned} c_1 &= \tanh \eta \sin(AT \cosh \eta), \\ c_2 &= -\frac{2i \tanh \eta}{\cosh \eta} \sin^2 \left[ \left( \frac{AT}{2} \right) \cosh \eta \right], \\ c_3 &= \left( \frac{\sinh^2 \eta [1 - \cos(AT \cosh \eta)]}{\cosh^2 \eta} - 1 \right). \end{aligned} \quad (3.6)$$

After this time, the relative magnitudes of the populations are not changed. In the adiabatic limit,  $\eta \rightarrow 0$ , the total population has been transferred to level  $|3\rangle$ , and the deviations from this ideal result behave as  $\eta^2$ . This polynomial dependence of the corrections to adiabaticity derives from our nonanalytic derivative in the coupling strengths, Eqs. (3.1) and (3.2). The result is similar to that found by Berry [21] and in the Ramsay-Schwinger model [22]. In the models (3.1) and (3.2), the first derivative is discontinuous, hence the asymptotic dependence  $T^{-2}$ . By a suitable choice of the pulse shapes, one can make the discontinuity appear in a higher derivative. Then the negative power of  $T$  increases,

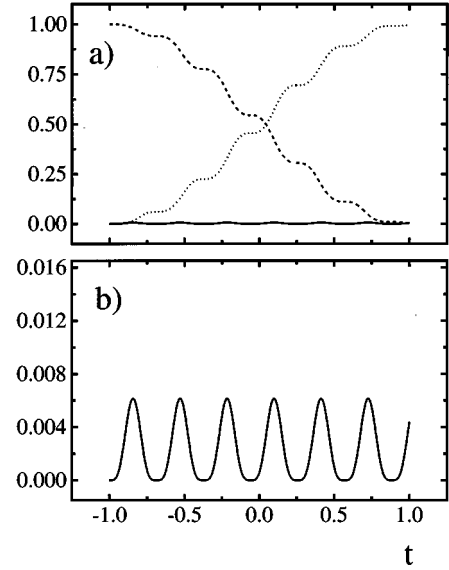


FIG. 4. The upper part (a) of the figure shows the population of the three levels coupled with the pulses of Fig. 3. Initially the population is on level 1 (dashed line) and finally mainly on level 3 (dotted line). The population on the intermediate level 2 is shown as a solid line. This population is magnified in part (b) of the figure. The behavior is strongly oscillatory, and the final population depends on the phase of the oscillations when the pulse ends. Time is given in parts of  $T/2$ .

but no fundamental change is seen. The asymptotic corrections to adiabaticity are still coming from the discontinuity in the pulse shapes.

In Fig. 4 we show the populations on the three levels as functions of time. We can see that the population on the intermediate level  $|2\rangle$  oscillates; toward the end of the interaction period its value depends on the phase. In the ideal case,  $\eta \rightarrow 0$ , the population on the intermediate level does not occur. The functions oscillate during the interaction period with the eigenvalues of the Hamiltonian (3.4), which is characteristic of all models of this type.

The model presented here is unrealistic, but it has the advantage that it does allow a full solution for all times. It also displays some of the features of the general case. The extension of the interaction functions is not expected to introduce any essential features, as we discussed in Sec. II. The nonadiabatic corrections go to zero in the adiabatic limit, albeit with a power-law behavior. The oscillatory phenomena have, in the adiabatic limit, a periodic dependence on the dimensionless parameter  $AT$ ; this makes the results of the intermediate level sensitive to the value of  $AT$ , which defines the phase of the oscillation when the interaction ends (see Fig. 4). For models with smooth interactions, this feature is expected to vanish.

## B. Exponential model

In this section we want to replace the simple nonanalytic pulse shapes (3.1) and (3.2) by smoothly varying shapes. To interpret the results with the concepts introduced in the previous model, we try to choose functions as similar as possible to those in that section. We set

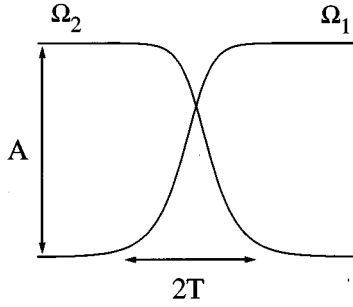


FIG. 5. The smooth exponential pulses imitating the features of the discontinuous behavior in Fig. 3.

$$\begin{aligned}\Omega_1^2(t) &= \frac{A^2}{1 + e^{-t/T}}, \\ \Omega_2^2(t) &= \frac{A^2}{1 + e^{+t/T}};\end{aligned}\quad (3.7)$$

the time behavior of these couplings is shown in Fig. 5. With these functions, we easily see that the amplitude in Eq. (2.7) becomes constant,  $\Omega_0 = A$ ; and for zero detuning, the Hamiltonian acquires for all times the form (3.4), with the nonadiabatic coupling being

$$\gamma = \frac{\dot{\theta}}{\sqrt{2}} = \frac{1}{2^{5/2}T \cosh(t/2T)}; \quad (3.8)$$

this is no longer a constant in time but turns on and off, smoothly imitating the behavior of the coupling in the preceding section. The only dimensionless parameter determining the behavior is the product  $AT$ , as before.

The variation of the populations with time in the exponentially coupled case is shown in Fig. 6. There appears a transient population on level  $|2\rangle$ , but this displays no oscillations and disappears smoothly. The populations on the levels  $|1\rangle$  and  $|3\rangle$  are exchanged in the expected adiabatic manner. The figure is close to adiabatic,  $A = 100$  and  $T = 1/30$ ; less than 0.6% of the population visits the intermediate state. If we choose parameters further from the adiabatic limit,  $A = 30$  and  $T = 1/30$ , we find the result in Fig. 7. Here nearly 10% of the population visits the intermediate state, and the remaining population of level  $|2\rangle$  is of the order of 1%. With the present coupling functions, i.e.,  $\Omega_1$  not turning off at infinity, the fraction of population left in states  $|1\rangle$  and  $|2\rangle$  remains coupled by a constant and executes Rabi oscillations, which are clearly seen in Fig. 7. The population on level  $|3\rangle$  is decoupled and stays constant.

To see the emergence of the adiabatic limit, we plot in Fig. 8 the nonadiabatic deviation from the ideal transfer, viz.,

$$\Delta P_3 = 1 - |c_3(\infty)|^2, \quad (3.9)$$

as a function of the adiabaticity parameter  $AT$ . We see that the semilogarithmic scales chosen suggest that there is an exponential disappearance of the nonadiabaticity in the ideal limit; in fact, the tail of the curve in Fig. 8 can be fitted to the expression

$$\Delta P_3 = 1 - 7.992 \exp(-6.281AT). \quad (3.10)$$

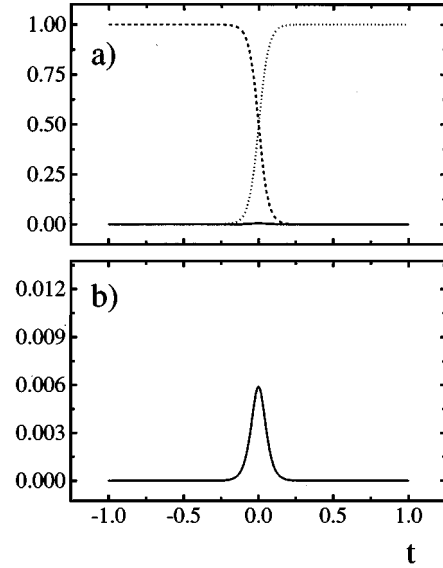


FIG. 6. The time evolution of the level populations induced by the pulses in Fig. 5. The representation is like that in Fig. 4. Part (a) shows level 1 (dashed), level 3 (dotted), and level 2 (solid). The last result is shown amplified in part (b). The adiabaticity parameter is  $AT = 3.3$ . The intermediate-level population is small and shows no oscillations. The time scale is chosen in a convenient way in this picture and the following ones.

This type of formula agrees with the results from the adiabatic theory of two-level systems [19]. Thus we may look for a theoretical approach that will reveal the relation.

We proceed to consider the equivalent two-level model according to Sec. II B. The exponential model parameters of the three-level system correspond exactly with those of Eq. (2.14), and with the functional dependence (3.8) we recognize in Eq. (2.14) the well-known Rosen-Zener Hamiltonian

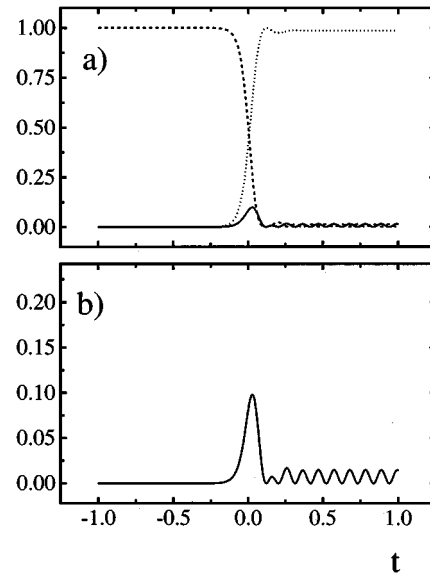


FIG. 7. The same as in Fig. 6 but with the adiabaticity parameter  $AT = 1$ . The adiabatic behavior is less ideal, and the population remaining on the coupled levels 1 and 2 performs Rabi oscillations because the coupling  $\Omega_1$  extends to infinity.

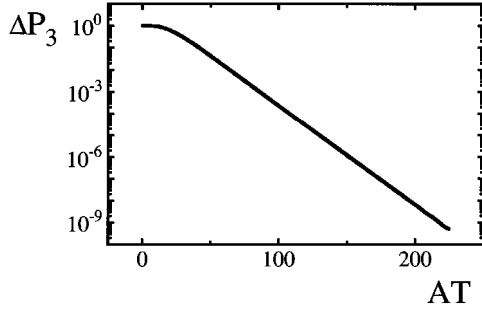


FIG. 8. The deviation from ideal behavior as a function of the adiabaticity parameter  $AT$ . The semilogarithmic plot shows that an adiabatic exponential region exists. This is verified from the analytic theory in the text.

$$H_{\text{RZ}} = \begin{bmatrix} -a & -i \frac{b}{\cosh(\pi t/\tau)} \\ i \frac{b}{\cosh(\pi t/\tau)} & a \end{bmatrix}; \quad (3.11)$$

with the initial conditions (2.15), the solution is [19]

$$|d_2(\infty)|^2 = \frac{\sin^2 b \tau}{\cosh^2 a \tau}. \quad (3.12)$$

After having identified the parameters in the Hamiltonian (3.11), we find the solution of the three-level problem (2.23) to be

$$|c_3(\infty)|^2 = \tanh^4(\pi AT). \quad (3.13)$$

This is an exact solution for our three-level problem with the exponential pulse shapes defined in Eq. (3.7). In the adiabatic limit  $AT \rightarrow \infty$ , this formula becomes

$$|c_3(\infty)|^2 \sim 1 - 8 \exp(-2\pi AT), \quad (3.14)$$

in excellent agreement with the numerical result in Eq. (3.10). The success of this type of asymptotic emergence of the adiabatic limit suggests that we also try the same type of analysis in other cases below.

In this section we have introduced a smooth ramp pulse that simulates the features of the nonanalytic trigonometric model of Sec. III A. The model chosen shows many ideal features: It contains no oscillatory behavior, it has a well-developed exponential asymptotic limit, and in addition its associated two-level model gives an exact analytic solution for all parameter values. There is only one significant dimensionless quantity in the model,  $AT$ , but this is characteristic of all ramp pulses with the same time scale and the same amplitude for the two pulses. We have investigated other simple ramp pulses of this type; the behavior does not differ significantly from that found in the present model. We do not expect the introduction of separate time scales and/or amplitudes for the two pulses to cause significant changes in the behavior of the solution. However, turning to the case of separated pulses, in the next section, we find a different type of behavior.

## IV. SEPARATED PULSES

### A. General considerations

We are now ready to consider pulses of finite duration, but we continue the resonant case  $\Delta = 0$ . Such pulses have earlier been used in both theoretical and experimental investigations; they vanish at both initial and final times. We thus introduce a general pulse-shape function  $f(x)$  such that

$$\lim_{x \rightarrow \pm\infty} f(x) = 0 \quad (4.1)$$

and

$$f(0) = 1. \quad (4.2)$$

If we now write

$$\begin{aligned} \Omega_1(t) &= Af\left(\frac{t-\tau}{T}\right), \\ \Omega_2(t) &= Af\left(\frac{t+\tau}{T}\right), \end{aligned} \quad (4.3)$$

we realize the counterintuitive pulse sequence for positive  $\tau$ ; see Fig. 2. For negative values of  $\tau$ , ordinary coherent pulse evolution is expected. Because the population probabilities on the different levels are dimensionless numbers, they can depend only on the two dimensionless parameters

$$\begin{aligned} \xi &= AT, \\ \zeta &= \tau/T. \end{aligned} \quad (4.4)$$

For the ramp pulses we had only one parameter  $\xi$ , and the adiabatic limit consists of this going to infinity; hence we call it the adiabaticity parameter. Here we have another essential parameter, too, and the genuine adiabatic limit arises when we let  $T$  go to infinity but keep  $(T/\tau)$  constant. In this case, all time variations scale in the same way and only one adiabatic parameter remains.

In the case when  $\tau$  is kept constant, we encounter a different phenomenon. When  $T$  increases, the pulse delay becomes less and less significant, and finally we expect the pulses to fall nearly on top of one another. To decide what to expect in this limit, we set  $\tau = 0$  in Eqs. (4.3). Then the time dependence factors out of Schrödinger's equation; and expressed in terms of the time variable  $\vartheta$ , defined through the relation

$$d\vartheta = f\left(\frac{t}{T}\right) dt, \quad (4.5)$$

the Hamiltonian becomes constant and can be solved trivially. Then the solution is found to display simple coherent oscillations in terms of the redefined time variable  $\vartheta$ , and no asymptotic behavior is expected. For pulse functions  $f(x)$ , the variable  $\vartheta$  is a monotonous function of  $t$ , and hence the transformation (4.5) is only a reparametrizing of the time axis.

From the argument above, we expect that by letting  $AT$  go to infinity without changing  $\tau$ , we eventually reach a

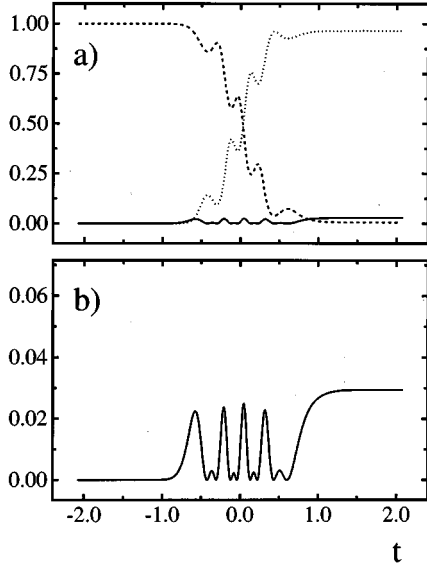


FIG. 9. The population behavior under the influence of two separated Gaussian pulses. The representation is like that in Figs. 4 and 6. The population is transferred from the initial level (dashed) to the final level (dotted), with some population occurring on the intermediate level (solid). This is shown magnified in part (b). The parameters  $A=20$  and  $T=0.5$ , and the pulse separation is  $\tau=0.35T$ . The behavior is not adiabatic. The pulses are too close; the population transfer is incomplete and oscillations are predominant.

region where coherent oscillations dominate the behavior. This will be investigated in the following for specific models.

The three-level system was shown in Sec. II B to be equivalent to a two-level one. In these cases, the adiabatic limit has been found to be dominated by the behavior of the adiabatic eigenvalue in the complex plane. The parameter (2.7) is defined to be nonnegative for all real times, but it may have complex zeroes  $t_c$  given by

$$\Omega_0(t_c)=0. \quad (4.6)$$

As shown by Davis and Pechukas [23], the zero nearest the real axis determines the adiabatic limit. We define the complex quantity

$$\Delta(t_c)=\int_0^{t_c}\Omega_0(t)dt. \quad (4.7)$$

With the initial condition (2.15), we expect to find the adiabatic limiting behavior

$$|d_1(\infty)|^2 \propto \exp[-2 \operatorname{Im}\Delta(t_c)]. \quad (4.8)$$

Without critically analyzing the validity of this asymptotic result, we test its applicability to the separated pulse problem in our systems.

### B. Exponential pulses

The STIRAP has been investigated theoretically mainly with Gaussian pulse shapes. We thus consider the case when the function in Eqs. (4.3) is given by

$$f(x)=\exp(-x^2). \quad (4.9)$$

For this pulse, the variables in the adiabatic representation are given by the adiabatic energy

$$\Omega_0^2(t)=2A^2\exp\left[-\frac{2}{T^2}(t^2+\tau^2)\right]\cosh\left(\frac{4t\tau}{T^2}\right) \quad (4.10)$$

and the nonadiabatic coupling

$$\dot{\theta}=\frac{2\tau}{T^2\cosh\left(\frac{4t\tau}{T^2}\right)}. \quad (4.11)$$

As in the adiabatic two-level cases, the zeroes of the energy are found to be singularities in the coupling. This is known to prevent a straightforward use of a stationary phase approximation to evaluate the transition probabilities.

In Fig. 9 we show the numerically evaluated populations on the three levels with the Gaussian coupling functions. Here we have the adiabaticity parameter  $\xi=AT=10$ , but the pulse separation is only  $\tau=0.35T$ . This is small enough to induce considerable coherent evolution, as discussed above, and the situation is found to give only incomplete population transfer to level 3; a large fraction of the population remains on level 2. In Fig. 10, the adiabaticity parameter is still only  $\xi=AT=12.5$ , but now the pulse spacing has been increased to  $\tau=0.6T$ . This slight change has improved the adiabaticity of the population transfer considerably; only the small intermediate population on level 2 displays clear oscillations. With an accuracy better than one per mille, we find the final population all on level 3 as desired; except for the oscillations, the behavior greatly resembles that shown in Fig. 6.

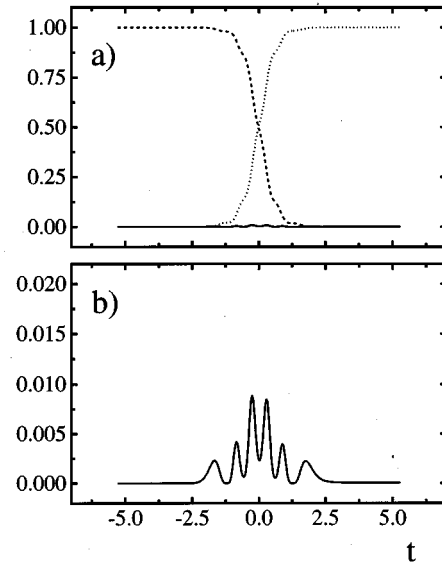


FIG. 10. The same as in Fig. 9, but now the pulse separation is increased to  $\tau=0.6T$ . The parameters are  $A=10$  and  $T=1.25$ . The degree of adiabaticity is no better than that of Fig. 9, but the increased pulse separation makes the behavior much closer to ideal. Only little population visits transiently the intermediate level, and hardly any remains. The populations still display oscillations like those in Fig. 4 even if the general behavior is similar to that in Fig. 6.

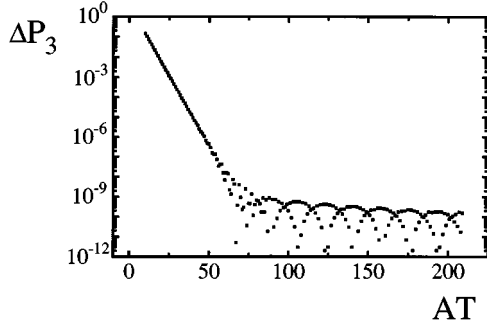


FIG. 11. Plots the deviation from ideal adiabaticity in the manner of Fig. 8, when we use Gaussian pulse shapes. The exponential region is seen to end for some value of  $AT$ , after which rapid oscillations are seen; they are not resolved in this figure. The picture is obtained for  $\tau=T$ ; for larger delays, the linear region becomes more extended, going down to  $10^{-10}$  around the values  $\tau=1.2T$ . The values in Table I are obtained from fits of lines to plots like these.

We find that the pulse separation in Fig. 10 gives good adiabaticity, in agreement with the results reported earlier [13].

To investigate the appearance of an asymptotic region we plot, for the pulse separation  $\tau=T$ , the deviation from adiabatic transfer  $\Delta P_3$ , Eq. (3.9), as a function of the adiabaticity parameter  $\xi=AT$  in Fig. 11. For numerical simplicity we have approached the adiabatic limit by letting  $A$  grow. The plot is chosen semilogarithmic to reveal an asymptotic region of the form

$$\Delta P_3(\xi) = 1 - \alpha e^{-\beta \xi}. \quad (4.12)$$

As we can see from the plot, the exponential behavior is followed up to  $\xi \approx 50$  over a decay by seven orders of magnitude. After this point, the coherent oscillations start to dominate and the asymptotic behavior breaks down. This agrees with our conclusions above; too much overlap between the pulses makes the coherent oscillation dominate. For pulse separations near the optimal adiabatic behavior,  $\tau > T$ ; the exponential region extends over an even much larger range of the parameter  $AT$ .

In the region where the exponential behavior is found, we may try to determine the exponent from the theory in Sec. IV A. The zero of the function (4.10) closest to the real axis is

$$t_c = i \frac{\pi T^2}{8\tau}. \quad (4.13)$$

When this is inserted into Eq. (4.8), we obtain a theoretical estimate for the exponent  $\beta$ . This may be compared with the one obtained from the numerical fit to the expression (4.12). This is again carried out in such a manner that  $\tau/T$  is kept constant, and the adiabatic limit is reached by increasing the amplitude  $A$ . The results are shown in Table I.

Table I confirms our conclusion that adiabatic transfer dominates the behavior for the pulse separation  $\tau > T$ . In this region unquestionable exponential dependence on the adiabaticity parameter is found. For closer pulses, too much coherent evolution occurs; for larger separation, the exponen-

TABLE I. Parameters for Gaussian pulses.

$\frac{2\tau}{T}$	$\beta$ (numeric)	$\beta$ (analytic)
2.0	0.3220	0.3238
2.2	0.2365	0.2370
2.4	0.1709	0.1717
2.6	0.1226	0.1230
3.0	0.0601	0.0605

tial region cannot be found because the total transfer of population becomes exceedingly small.

### C. Secant pulses

In the previous section we considered some features of the separated pulse system with Gaussian shapes. To decide if the features observed are generic or characteristic of the Gaussian only, we look at another popular pulse shape. We choose the hyperbolic secant pulse function

$$f(x) = \text{sech}(x) \quad (4.14)$$

instead of (4.9). The adiabatic energy then becomes

$$\begin{aligned} \Omega_0^2(t) &= A^2 \left[ \text{sech}^2\left(\frac{t-\tau}{T}\right) + \text{sech}^2\left(\frac{t+\tau}{T}\right) \right] \\ &= 2A^2 \text{sech}^2\left(\frac{t-\tau}{T}\right) \text{sech}^2\left(\frac{t+\tau}{T}\right) \\ &\quad \times \left[ \cosh^2\left(\frac{t}{T}\right) \cosh^2\left(\frac{\tau}{T}\right) + \sinh^2\left(\frac{t}{T}\right) \sinh^2\left(\frac{\tau}{T}\right) \right]. \end{aligned} \quad (4.15)$$

The nonadiabatic coupling is

$$\begin{aligned} \dot{\theta} &= \frac{\sinh\left(\frac{2\tau}{T}\right)}{T \left[ \cosh^2\left(\frac{t-\tau}{T}\right) + \cosh^2\left(\frac{t+\tau}{T}\right) \right]} \\ &= \frac{\sinh\left(\frac{2\tau}{T}\right)}{T \left[ 1 + \cosh\left(\frac{2t}{T}\right) \cosh\left(\frac{2\tau}{T}\right) \right]}. \end{aligned} \quad (4.16)$$

As in the previous case, we find that the zeroes of  $\Omega_0(t)$  are poles of the coupling. Both the coupling (4.11) and (4.16) vanish exponentially for  $t \gg T$ . Thus some similarity in their behaviors is expected. Numerical investigations show that the population behaves much in the manner shown in Fig. 10 for the Gaussian case. The tails of the secant pulses do, however, fall off more slowly, and consequently larger pulse separations  $\tau$  are needed to avoid excessive coherent evolution.

In Fig. 12, we show the behavior of the deviation from adiabaticity  $\Delta P_3$  as a function of  $AT$ , as in Fig. 11. The pulse separation is here  $\tau=3.5T$ , and still an adiabatic exponential region is barely visible. The numerical work to deter-

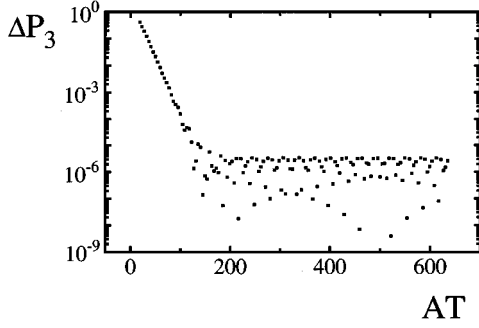


FIG. 12. A plot like that in Fig. 11 but with hyperbolic secant pulse shapes. The pulse separation has to be larger,  $\tau=3.5T$ , and the linear region is less extended. Fits of lines to the linear parts give the parameters in Table II.

mine the parameters of the fit to the form (4.12) is much more difficult than for the Gaussian case, but the parameter  $\beta$  can be extracted. Again, we can compare this to the analytic approximation from Eq. (4.8).

Closest to the real axis, we find the zero of the adiabatic energy  $\Omega_0(t)$  in Eq. (4.15) to be

$$t_c = iT \arctan \left[ \coth \left( \frac{\tau}{T} \right) \right]. \quad (4.17)$$

This can be used in Eq. (4.7) to obtain the analytic approximation to  $\beta$ . This is compared with the numerically obtained value in Table II.

Table II shows that for the secant pulses also, we do find a region where the asymptotic pole approximation gives a good representation of the data. However, the required pulse separation is considerably larger than in the Gaussian case. This we ascribe to the slower decay rate of the secant pulses. Nevertheless, the general pattern of the behavior is the same. After the exponential region, from some value of  $AT$  onward the simple behavior breaks up into oscillations; compare Figs. 11 and 12. The oscillations take place over the range of  $AT \approx 1$ , and hence the pattern is not resolved in the figures.

#### D. Conclusions

For two types of separated pulses that vanish at infinity, we have found very similar behavior. When the coupling amplitude is increased, an asymptotic exponential regime first emerges, which for large enough amplitudes breaks up into a rapidly oscillating pattern. When the pulse separation becomes a larger fraction of the pulse width, the exponential region becomes more extended. We interpret this to mean that the increased pulse amplitude stresses the importance of

TABLE II. Parameters for secant pulses.

$\frac{2\tau}{T}$	$\beta$ (numeric)	$\beta$ (analytic)
7.0	0.0997	0.1024
8.0	0.0608	0.0621
9.0	0.0373	0.0376
10.0	0.0227	0.0228

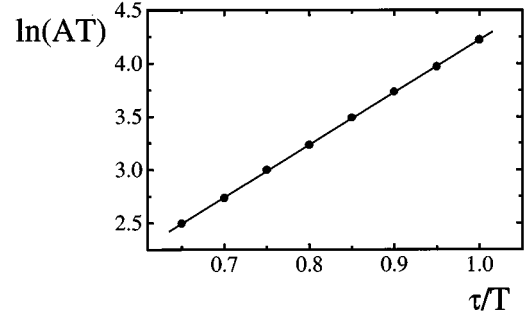


FIG. 13. In plots like Fig. 11, we determine the critical value of the adiabaticity parameter  $(AT)_{\text{crit}}$  for which the linear behavior breaks up into oscillations. This is plotted as a function of the pulse separation parameter  $(\tau/T)$  for Gaussian pulses. The plot shows that an exponential dependence is obvious.

the pulse overlap leading to enhanced coherent evolution. This stops the exponential decay and lets the oscillation behavior dominate.

In this paper we have applied the Davis-Pechukas result (4.8) totally uncritically. In its derivation, however, a time integration path from  $-\infty$  to  $+\infty$  is deformed to the complex zero of the adiabatic energy. The contribution from this zero then dominates the behavior in the adiabatic regime. The procedure assumes that no trouble is caused by the behavior of the functions at infinity. In the present cases this is not true. In both models investigated, the Gaussian case and the hyperbolic secant, Eqs. (4.10) and (4.15), the adiabatic energies show complicated behavior near  $\pm i\infty$ . Both can take arbitrarily large values here, and this behavior may invalidate the asymptotic analysis. If we modify the pulses to make the adiabatic energy well behaved at infinity, the oscillatory regime for large  $\xi$  seems to be eliminated. We offer no theoretical explanation for this observation.

The value of the parameter  $\xi = AT$ , at which the exponential decrease ceases, is expected to depend on the pulse delay-to-duration ratio  $\zeta = \tau/T$ . This can be extracted from the data in Figs. 11 and 12. The linear fit to the decay part is extended until it meets a line through, e.g., the peaks of the oscillating part. This crossing is chosen as the critical value for the adiabaticity parameter  $\xi_c$ . This is then plotted semi-logarithmically against  $\zeta$  for the Gaussian and secant pulses in Figs. 13 and 14, respectively. With good accuracy, the behavior is found to fit the equation

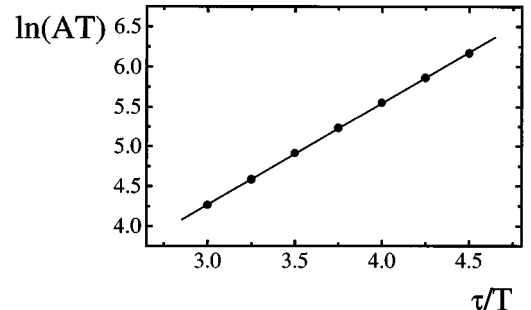


FIG. 14. The same plot as in Fig. 13 but for the hyperbolic secant pulse. The data are obtained from plots like that in Fig. 12. Also here the exponential dependence is well verified.

TABLE III. Parameters in Eq. (4.18).

	Gaussian pulse	Secant pulse
$\kappa$	0.49	1.57
$\mu$	4.93	1.27

$$\xi_c = \kappa e^{\mu \zeta}. \quad (4.18)$$

In Table III we give the parameters obtained numerically for the two pulse shapes investigated. We have no analytic explanation for this observed relation. The good fits provided by Figs. 13 and 14 suggest that the behavior (4.18) is generic for a certain class of pulse shapes, but lacking a theoretical explanation we are unable to suggest how general the result is.

## V. DISCUSSION

In this paper we have considered the nonadiabatic corrections to the well-known adiabatic population transfer connected with a counterintuitive pulse sequence for a three-level system. When the intermediate level is at resonance, we utilize a representation of the problem in terms of a two-level Hamiltonian. We point out that the conventional configuration of separated pulses can be replaced by two ramp pulses approaching constant values at infinity. The adiabatic part of the transfer is the same.

We illustrate the use of the ramp pulse by two examples: One is a trivial discontinuous trigonometric model, which is analytically solvable, but because of the discontinuous derivatives all nonadiabatic corrections occur as simple powers of the inverse of the time scale. The model does, however, illustrate the use of ramp pulses. The second example consists of smooth exponential pulses. They have been chosen such that the algebraic structure of the problem simplifies in the adiabatic basis. In fact, the associated two-level problem becomes solvable, and the asymptotic behavior in the adiabatic limit can be verified to agree with that which we extracted from a numerical treatment. This suggests that the Davis-Pechukas asymptotic analysis can be applied to the two-level formulation of the three-level problem.

We then proceed to consider the situation with separated pulses, which decay to zero at  $\pm\infty$ . We investigate Gaussian and hyperbolic secant pulses and look for regions where exponential asymptotics occur. For pulses that are sufficiently

separated in time, such regions are found; but in contrast to expectations, they end when the adiabaticity parameter grows too large and are replaced by rapidly oscillating solutions. We ascribe this behavior to a takeover by the coherent oscillations, which derive from the region where the pulses overlap significantly. When the pulse amplitude is increased, this overlap grows.

We determine the position of the crossover between exponential and oscillatory behavior numerically and find an unexpected exponential relation. Thus increasing the pulse separation rapidly pushes the crossover to larger values of the adiabaticity parameter and consequently smaller actual values of the nonadiabatic corrections. Too large separations, however, will eventually destroy the effect because the pulses overlap only at negligibly small amplitudes. Hence there is an optimum separation for adiabatic transfer. We have no analytic theory to explain these features of the behavior.

For a resonant intermediate level, the three-level problem is equivalent with an associated two-level problem. Much work has been carried out on adiabatic behavior and nonadiabatic corrections in such systems. However, the cases occurring with counterintuitive separated pulses are of a type not usually discussed for two levels. As seen from Eq. (2.20), the total Hamiltonian disappears at both time limits  $\pm\infty$ . The two levels involved are then degenerate, and all nonadiabatic transfer between them takes place with separated adiabatic energies. The difference between the ordinary and the counterintuitive sequences derives from whether the levels become coupled before they separate or separate before they couple. In the case of the two-level situation, this question seems not to have been investigated before. Our discussion of the three-level system can be rephrased to deal with the associated two-level situation directly. We feel that considerable work is still needed to understand this aspect of the situation.

In conclusion, the adiabatic behavior of the three-level system has been found to exhibit many unexpected and challenging features. Some of these we have been able to relate to exact solutions and analytic approximations. The latter have, however, been introduced *ad hoc* without derivation. Many results are based on numerical evidence only. As this is afflicted with accuracy problems and insufficient generality, we would really like to see more detailed investigations of the analytic behavior of the systems discussed in this paper. We hope that such work will be possible in the future.

- 
- [1] F. T. Hioe, Phys. Lett. A **99**, 150 (1983).
  - [2] J. Oreg, F. T. Hioe, and J. H. Eberly, Phys. Rev. A **29**, 690 (1984).
  - [3] C. E. Carroll and F. T. Hioe, Phys. Rev. A **36**, 724 (1987).
  - [4] C. E. Carroll and F. T. Hioe, J. Opt. Soc. Am. B **5**, 1335 (1988).
  - [5] C. E. Carroll and F. T. Hioe, J. Phys. B **22**, 2633 (1989).
  - [6] C. E. Carroll and F. T. Hioe, Phys. Rev. A **42**, 1522 (1990).
  - [7] J. R. Kuklinski, U. Gaubatz, F. T. Hioe, and K. Bergmann, Phys. Rev. A **40**, 6741 (1989).
  - [8] B. W. Shore, K. Bergmann, J. Oreg, and S. Rosenwaks, Phys. Rev. A **44**, 7442 (1991).
  - [9] B. W. Shore, K. Bergmann, and J. Oreg, Z. Phys. D **23**, 33 (1992).
  - [10] B. W. Shore, K. Bergmann, A. Kuhn, S. Schiemann, and J. Oreg, Phys. Rev. A **45**, 5297 (1992).
  - [11] A. Kuhn, G. W. Coulston, G. Z. He, S. Schiemann, and K. Bergmann, J. Chem. Phys. **96**, 4215 (1992).
  - [12] J. Oreg, K. Bergmann, B. W. Shore, and S. Rosenwaks, Phys. Rev. A **4**, 4888 (1992).

- [13] U. Gaubatz, P. Rudecki, S. Schiemann, and K. Bergmann, *J. Chem. Phys.* **92**, 5363 (1990).
- [14] S. Schiemann, A. Kuhn, S. Steuerwald, and K. Bergmann, *Phys. Rev. Lett.* **71**, 3637 (1993).
- [15] P. Pillet, C. Valentin, R.-L. Yuan, and J. Yu, *Phys. Rev. A* **48**, 845 (1993).
- [16] M. V. Danileiko, V. I. Romanenko, and L. P. Yatsenko, *Opt. Commun.* **109**, 462 (1994).
- [17] T. Nakajima, M. Elk, J. Zhang, and P. Lambropoulos, *Phys. Rev. A* **50**, R913 (1994).
- [18] M. Elk, *Phys. Rev. A* **52**, 4017 (1995).
- [19] B. M. Garraway and K.-A. Suominen, *Rep. Prog. Phys.* **58**, 365 (1995).
- [20] B. L. van der Waerden, *Group Theory and Quantum Mechanics* (Springer-Verlag, Berlin, 1974), Chap. 3, Sec. 19.
- [21] M. V. Berry, *J. Phys. A* **15**, 3693 (1982).
- [22] S. Stenholm, *Quantum Dynamics of Simple Systems*, Lectures at the 44th Scottish Universities' Summer School in Physics, 1994 (Institute of Physics, Bristol, in press).
- [23] J. P. Davis and P. Pechukas, *J. Chem. Phys.* **64**, 3129 (1976).
- [24] J.-T. Hwang and P. Pechukas, *J. Chem. Phys.* **67**, 4640 (1977).